Degeneracy in the Inference of Phase Transitions in the Neutron Star Equation of State from Gravitational Wave Data

Carolyn A. Raithel [*] and Elias R. Most [†]
School of Natural Sciences, Institute for Advanced Study, 1 Einstein Drive, Princeton, New Jersey 08540, USA; Princeton Center for Theoretical Science, Jadwin Hall, Princeton University, Princeton, New Jersey 08544, USA and Princeton Gravity Initiative, Jadwin Hall, Princeton University, Princeton, New Jersey 08544, USA

(Received 8 August 2022; revised 19 December 2022; accepted 10 April 2023; published 18 May 2023)

Gravitational wave (GW) detections of binary neutron star inspirals will be crucial for constraining the dense matter equation of state (EOS). We demonstrate a new degeneracy in the mapping from tidal deformability data to the EOS, which occurs for models with strong phase transitions. We find that there exists a new family of EOS with phase transitions that set in at different densities and that predict neutron star radii that differ by up to ~500 m but that produce nearly identical tidal deformabilities for all neutron star masses. Next-generation GW detectors and advances in nuclear theory may be needed to resolve this degeneracy.

DOI: 10.1103/PhysRevLett.130.201403

Introduction.—Gravitational wave (GW) events offer exciting prospects to constrain the properties of dense matter (see, e.g., Refs. [1–4]). In particular, the GW signal emitted during the final orbits of two colliding neutron stars contains imprints of the tidal deformability parameter $\tilde{\Lambda}$ that can be related to the properties of dense matter in terms of the equation of state (EOS) (see, e.g., Refs. [5–13]). In practice, this inference is limited by the sensitivity to which the tidal deformability can be constrained. For example, for the GW170817 event, $\tilde{\Lambda}$ was constrained to 300^{+420}_{-230} at 90% confidence [14], which has been translated to constraints on the neutron star radius of $10 \lesssim R \lesssim 13$ km (see, e.g., Refs. [5,7–11]).

When advanced LIGO reaches its fifth observing campaign (called "A+"), it is expected that the tidal deformability will be able to be constrained to uncertainties of $\sigma_{\tilde{\Lambda}} \approx 46$ at 68% confidence, for a GW170817-like event. With next-generation (XG) GW detectors, these bounds on $\tilde{\Lambda}$ will be further improved, leading to anticipated constraints of $\sigma_{\tilde{\Lambda}} < 8$ from the inspiral GW signal for a similar event and $\sigma_{\tilde{\Lambda}} \approx 1$–4 for a population of mergers observed with XG detectors, depending on the merger rate [15]. From the usual quasiuniversal relations that map tidal deformabilities to the neutron star radius (see, e.g., Refs. [10,11,16–18]), one would typically assume that small uncertainties in $\sigma_{\tilde{\Lambda}}$ directly translate to tight constraints on R, potentially to 50–200 m accuracy [4], assuming that dynamical tides are correctly accounted for in the extraction of $\tilde{\Lambda}$ [19,20]. In all of these efforts, a key goal is to determine what relevant degrees of freedom exist in the dense-matter cores of neutron stars—for example, whether there exists a phase transition (e.g., to deconfined quark matter), what the nature of the phase transition is, and at what densities this transition occurs (see, e.g., Refs. [21–28]).

In this work, we identify a new degeneracy in the mapping from the tidal deformability to the neutron star EOS, which arises specifically for models with strong phase transitions at densities around nuclear saturation. We demonstrate this degeneracy with an example Bayesian inference of the EOS, using mock tidal deformability data generated from an EOS with a first-order phase transition. For the sensitivity of the A + LIGO configuration, we find that it will be difficult to differentiate between certain classes of EOSs that have first-order phase transitions setting in at different densities and that even models with no phase transition at all can mimic the same tidal deformability data. With the sensitivity of proposed XG detectors, the constraints on the EOS remain broad, but the degeneracy between these different phase transitions starts to resolve.

Using these inference results as motivation, we show that it is generically possible to construct EOS models that have phase transitions that set in at significantly different densities—leading to differences in the predicted stellar radii of ~300 m—but that predict nearly identical tidal deformabilities across the entire range of astrophysically observed neutron star masses (corresponding to, e.g., absolute differences of $\Delta\Lambda \lesssim 5$ and fractional differences $\lesssim$1%–2% for intermediate-mass stars). Given the similarity of these models' macroscopic features, despite their significant differences in underlying microphysics, we refer to these EOSs as "tidal deformability doppelgängers."

We demonstrate that, with additional input from nuclear theory to extend the crust EOS to supranuclear densities (see, e.g., Refs. [29–32]), combined with the sensitivity of XG GW observatories, it may be possible to break the

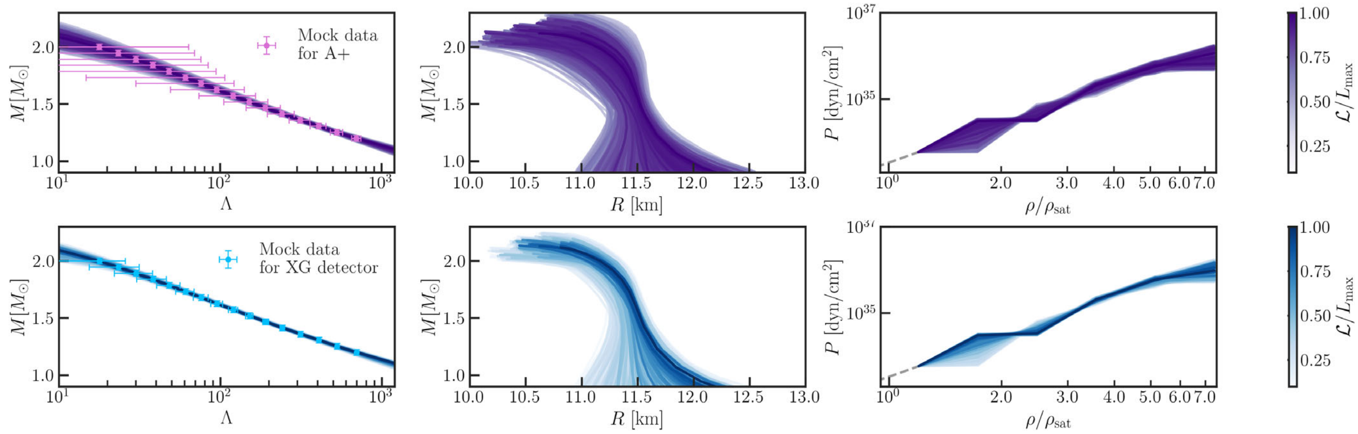

FIG. 1. Top row (in purple): Bayesian inference of the EOS for mock data, generated assuming Gaussian errors in tidal deformability, Λ, for LIGO at the sensitivity of its fifth observing run (A+), for a series of GW170817-like events ($\sigma_\Lambda = 46$). From left to right, we show the most likely tidal deformability curves, mass-radius curves, and EOSs inferred in our Bayesian inference. To highlight the degeneracy of the solutions, we randomly sample curves from the 68% confidence interval and color them according to their posteriors, relative to the most likely solution. Bottom row (in blue): an identical inference, but with Gaussian errors in Λ for the proposed XG detector Cosmic Explorer ($\sigma_\Lambda = 8$).

degeneracy when inferring strong phase transitions. The degeneracy will be easiest to break for low-mass neutron star binaries, if they exist in astrophysical populations. At present, however, this degeneracy cannot be resolved from GW data alone, and the inference of at least some families of phase transitions will be highly sensitive to the choice of priors assumed.

Inferring strong phase transitions from GW data.—We begin by introducing the degeneracy with a sample Bayesian inference of the EOS from mock GW data, following the statistical framework outlined in Ref. [33]. In our inference scheme, we assume that the crust EOS (ap3 [34]) is known perfectly to a fiducial density ρ_0, which we set here to be $1.2\rho_{\rm sat}$, where $\rho_{\rm sat} = 2.7 \times 10^{14}$ g/cm^3 is the nuclear saturation density. At higher densities, we parametrize the uncertainty in the EOS using five piecewise polytropic segments. When performing our inference, we impose a set of minimal requirements—namely, causality, stability, and the ability to support massive ($2.01M_\odot$) neutron stars—and we sample uniformly in the pressure. Finally, we also require that the maximum mass predicted by the EOS not exceed $2.3M_\odot$, in order to be consistent with inferences from GW170817 and its electromagnetic counterpart [35–39].

For the example inferences, we construct a series of mock tidal deformability data which were generated from an EOS that has a strong, first-order phase transition starting at $1.7\rho_{\rm sat}$. This EOS (which is shown as the dark blue curve in the middle row in Fig. 2) predicts the radius of a $1.4M_\odot$ neutron star to be $R_{1.4} = 11.6$ km and the tidal deformability at the same mass to be $\Lambda_{1.4} = 257$, consistent with current astrophysical constraints [9,14,40–48].

In the first example inference, we assign Gaussian errors to the tidal deformabilities based on the projected sensitivity of the LIGO detectors in their fifth observing run (A+). We optimistically assume that the A+ detectors observe 16 GW170817-like events, spaced evenly in mass across the entire range of astrophysically observed neutron star masses (i.e., from 1.2 to $2M_\odot$). (We consider the range of astrophysical neutron star masses to range from the lightest observed radio pulsar at $1.17M_\odot$ [49] to $2.01M_\odot$ [50,51]. Both quoted values correspond to the 1σ lower limit on the masses. We note that the 90% lower limit on the secondary mass for GW170817 was also $1.17M_\odot$ and that no lighter GW sources have yet been detected [52]. In general, the differences in the tidal deformability are largest at low masses, so taking the lower limit on the lowest mass considered provides the most conservative estimates possible for the degeneracies discussed in this Letter.) For such a scenario, the anticipated 1σ-measurement uncertainties in the tidal deformability would be $\sigma_\Lambda = 46$ [15]. We additionally assume that the masses are tightly constrained with Gaussian uncertainties of $0.025M_\odot$. (For simplicity, we also assume that these are equal mass binaries, so that the component tidal deformabilities are constrained directly. We explore the impact of unequal mass ratios on the degeneracy between these tidal deformabilities in Supplemental Material [53].)

We show the resulting constraints in the top row in Fig. 1 (in purple). In this figure, we include only samples drawn from the 68% confidence interval for visual clarity, and we color these according to their normalized posteriors. We find that, even with this optimistic set of mock data, we are able only to constrain the radius of a $1.4M_\odot$ neutron star to within 500 m and the pressure at $1.7\rho_{\rm sat}$ to within a factor of 5.8×, at 68% confidence. Moreover, as the color shading indicates, there are models on either edge of this broad uncertainty band that give comparably good posteriors. For example, models with a strong phase transition that sets in at lower densities ($1.2\rho_{sat}$) or higher densities ($1.7\rho_{sat}$) fit the data comparably well, as does an EOS that goes right through the middle of this uncertainty band with no phase transition at all. In short, we are not only unable to recover our initial EOS, but are also unable to rule out or confirm the presence of exotic nuclear phases, such as deconfined quark matter.

To further illustrate this degeneracy, we consider two example EOSs drawn from opposite edges of this uncertainty band. We show these EOSs in the middle row in Fig. 2, where the dark blue curve shows the EOS model used to generate the mock data and the light blue curve represents a separate EOS sampled in our inference. Despite the fact that these models predict first-order phase transitions at different densities and accordingly differ significantly in their supranuclear pressures, they fit the data similarly well with a Bayes factor of 1.9, indicating insufficient evidence to tell them apart [71].

This presents a significant degeneracy in the mapping from tidal deformability measurements to the underlying EOS. It has previously been shown that changing the crust EOS (at densities below 10^{14} g/cm^3) can change the radius without significantly affecting the tidal deformabilities [72]. Here, however, we find that large differences in the EOS at *supranuclear* densities may also be indistinguishable,

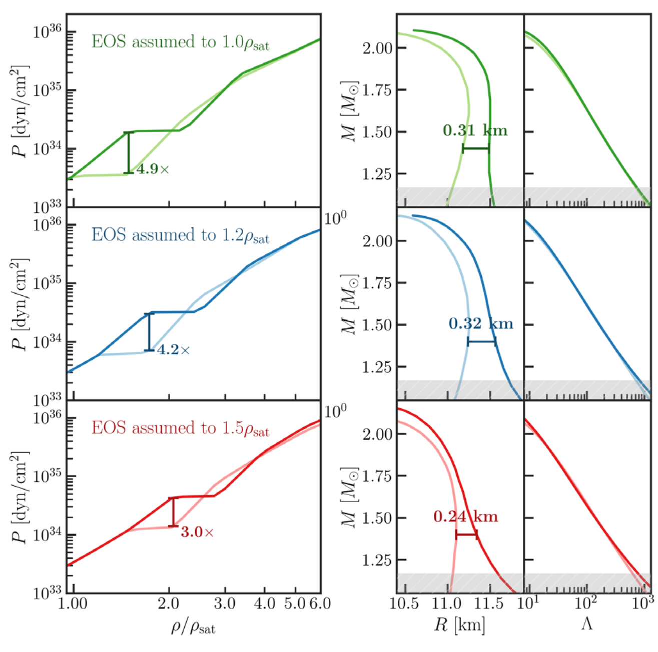

FIG. 2. Example pairs of EOS models that undergo a first-order phase transition at significantly different densities (40% fractional difference) and yet produce nearly identical tidal deformability curves. From left to right, we show the EOS models, their corresponding mass-radius relations, and their corresponding tidal deformability curves. Each pair of EOS models was constructed assuming perfect knowledge of the crust EOS to ρ_{sat} (top row, in green), $1.2\rho_{sat}$ (middle row, in blue), or $1.5\rho_{sat}$ (bottom row, in red).

even with optimistic A+ data observed across a wide range of masses.

In order to understand the sensitivity of this degeneracy to the measurement uncertainties, we perform a second Bayesian inference with an identical setup, but now assuming Gaussian errors on the tidal deformability measurements of $\sigma_\Lambda = 8$. These smaller errors on Λ correspond to the projected measurement uncertainty for the proposed XG detector Cosmic Explorer [73], for a GW170817-like event [15]. The results of this inference are shown in the bottom row in Fig. 1 (in blue). Again, we find a large spread in the inferred $R_{1.4}$ of ~500 m and in the pressure at $1.7\rho_{sat}$ of 5.7×, at 68% confidence. However, in this case, we see that the data have more discerning power for the most extreme EOS models in our inferred sample, as indicated by the gradient in colors.

To illustrate this point, we again consider the two example EOSs from the middle row in Fig. 2, which now have a Bayes factor of 3.3 for the XG data, indicating "substantial" evidence [71] in favor of the dark blue model (which was used to generate the mock data). Interestingly, the lowest-mass data points are the most constraining: For example, if we excise the mock data point at $1.2M_\odot$, then the Bayes factor between these models for the remaining data is only 1.6, which is insufficient evidence to select the correct EOS. This suggests that, if low-mass neutron star binaries exist in nature, they may be particularly powerful for resolving this degeneracy. We discuss this point further below.

In principle, with even one year of observations with Cosmic Explorer, we can expect tighter constraints on the tidal deformability than assumed here, of potentially $\sigma_\Lambda \approx 1$–4, depending on the astrophysical merger rate [15]. With such sensitivity—in particular, if combined with further input from nuclear theory—it will become possible to distinguish between these EOS models with higher confidence, as we show in the following section.

Finally, we note that we have taken very broad priors in this analysis (namely, flat priors on the pressure with minimal additional physical constraints). We make this choice in order to clearly demonstrate the constraining power of these mock GW data. Additional priors on the sound speed or on the likelihood of phase transitions in the EOS would readily differentiate between the inferred EOSs shown in Fig. 1. Indeed, we performed an additional set of inferences with more informative priors, and we find that the inclusion of even a weak prior penalizing variations in the sound speed acts to restrict the uncertainty bands in Fig. 1 but that such a prior can also bias the inference to select the incorrect EOS, even in the limit of high-quality XG data observed across a range of masses (for details, see Supplemental Material [53]). This suggests a strong sensitivity of such inferences to the choice of priors, for at least some regions of the EOS parameter space where the doppelgänger degeneracy is significant. In summary, these results demonstrate—for the first time—the limitations of current GW data in distinguishing between certain classes of EOS models with strong, supranuclear phase transitions, from the data directly.

Impact on future gravitational wave detections.—In order to understand this degeneracy in more detail, we construct several example pairs of EOS models that mimic the features identified in Fig. 1. Because of their almost identical tidal deformabilities despite large differences in their EOSs, we refer to these models as *tidal deformability doppelgängers*.

We show these "doppelgänger " EOSs in Fig. 2. The top row (in green) shows a pair of EOSs where the crust EOS is assumed to be known perfectly up to $\rho_{\rm sat}$, and the phase transition is allowed to set in soon thereafter. In the middle row (in blue), we show an example where the crust EOS is assumed to $1.2\rho_{\rm sat}$; these models correspond to the extreme edges of our 68% confidence band inferred in Fig. 1, as discussed in that section. Finally, in the bottom row (in red), we show an example pair of doppelgängers where the crust EOS is assumed to be known to $1.5\rho_{\rm sat}$. In all cases, we find that it is possible to construct pairs of EOS models that have very different microphysics—with first-order phase transitions that set in at significantly different densities and which accordingly predict neutron star radii that differ by ~300 m—and yet that predict tidal deformability curves that are nearly identical across the entire range of astrophysically observed masses.

We note that, although these are phenomenological models, the qualitative features are similar to more realistic calculations of EOSs with first-order phase transitions to deconfined quark matter (see, e.g., Refs. [74–76], and references therein). The difference in the transition densities in Fig. 2 can, thus, be associated with a difference in the deconfinement transition densities for these models or, more generally, with the onset densities for an exotic new degree of freedom.

Although the tidal deformability curves in Fig. 2 are very similar for a given pair of models, they are not perfectly identical. We show the differences in Λ for each of these pairs of models in Fig. 3, where, for reference, we also include estimates of the differences in Λ that could be resolved at 68% confidence for a population of neutron star mergers observed for one year with the sensitivity of current and upcoming detectors. These sensitivity estimates are shown with the vertical green band for aLIGO, in orange for A+, and in blue for Cosmic Explorer [15].

We find that, in general, the differences in Λ for any of these EOSs are most significant at low masses, consistent with the findings of the previous section. In addition, as the crust EOS is assumed to higher densities, the differences in Λ become more significant. For example, if the crust EOS is assumed to be known to $\rho_{\rm sat}$ ($1.5\rho_{\rm sat}$), we will likely need the sensitivity of Cosmic Explorer (A+, for a population of low-mass neutron star binaries) to distinguish the tidal deformabilities for this example, based on GW data alone. Thus, adopting stronger nuclear input—in terms of the density to which the crust EOS is assumed—can help to resolve this tidal deformability degeneracy. In summary, the most constraining data will likely come from low-mass neutron star binaries, which may even be able to resolve this degeneracy with current GW detectors, if combined with sufficient input from nuclear theory at supranuclear densities.

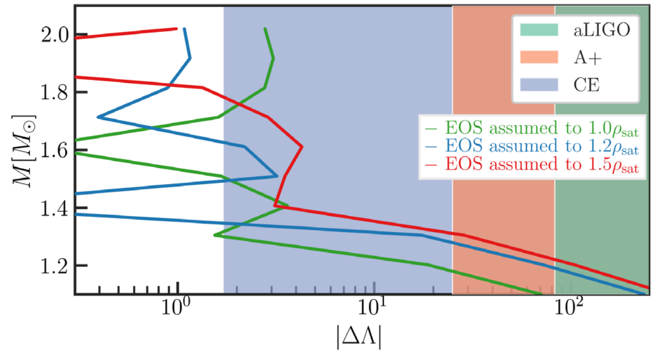

FIG. 3. Absolute differences in the tidal deformability Λ between each pair of doppelgängers shown in Fig. 2. As the crust EOS is assumed to higher densities, the tidal deformability curves become more distinct, with the largest differences emerging at low masses. The vertical shaded bands indicate the expected 68%-measurement uncertainty in Λ for a population of neutron star mergers observed over one year with the sensitivity of LIGO at design sensitivity (aLIGO), the anticipated sensitivity of LIGO during its fifth observing run (A+), and the proposed XG detector Cosmic Explorer (CE) [15].

We note that our discussion here focuses on a few illustrative examples, in order to discuss the implications for inferences from current and upcoming observations. We investigate the ubiquity of these doppelgängers and their full parameter space in a separate work [77].

Prospects for postmerger GWs.—In addition to providing tighter constraints on the tidal deformability of inspiraling neutron stars, another exciting prospect of XG detectors is the possibility of capturing the postmerger GW emission (see, e.g., Refs. [78–80]). Much work has been devoted to understanding the connection of EOS models to the postmerger frequency spectrum. These quasiuniversal relations rely to a large extent on correlations between the dominant frequency f_2 and the tidal deformabilities or radii of cold neutron stars (see, e.g., Refs. [81–91]). In particular, several works have investigated the possibility of constraining strong phase transitions this way [92–98].

To investigate this scenario, we perform binary neutron star merger simulations for two extreme pairs of doppelgänger EOSs, where the crust EOS is assumed only to $0.5\rho_{\rm sat}$. In one pair of doppelgänger EOSs, the characteristic radii are $R_{1.4} = 10.8$ and 11.2 km, similar to the examples shown in Fig. 2. We also construct a second pair of doppelgängers that are significantly stiffer, such that they predict characteristic radii of $R_{1.4} = 12.8$ and 13.2 km, yet differ by $\Delta\Lambda_{1.4} < 1$. We extend these zero-temperature, EOSs to finite temperatures and arbitrary compositions using the framework of Ref. [99] and perform merger simulations for each EOS using GW170817-like binary parameters. Two of these fully finite temperature models have been simulated previously [91,100], and the numerical setup [101,102] of our simulations here is identical to that work [100]; we provide key details in Supplemental Material [53].

From these simulations, we extract the peak frequencies of the postmerger GW emission and find that they are nearly indistinguishable for a given pair of doppelgängers. For the $R_{1.4} = 10.8$ and 11.2 km pair of models, we find $f_2 = 3.39$ kHz in both cases; while for the $R_{1.4} = 12.8$ and 13.2 km pair of models, $f_2 = 2.71$ and 2.65 kHz, respectively.

These results are consistent with the predictions of existing quasiuniversal relations, to within the numerical uncertainties in f_2, which we conservatively estimate to be at the 10% level [103]. In particular, the doppelgängers do not violate reported quasiuniversal relations between f_2 and the radius of a $1.8M_\odot$ star [90,91] or with the tidal deformability [104]. For additional discussion, see Supplemental Material [53].

In summary, to within the current uncertainties of numerical simulations—which may also be affected by systematic uncertainties in finite-temperature [105–107] and neutrino physics [108–111]—we find that the postmerger peak frequencies may not be able to differentiate between the strong phase transitions of some doppelgänger models. However, the field is likely to progress significantly by the XG era.

Summary.—In this work, we have identified a new degeneracy in the mapping from tidal deformability data to the underlying EOS, which arises for models with strong phase transitions. We find that certain families of EOS models, which have phase transitions that set in at significantly different densities and which predict radii that differ by ~300 m, can predict tidal deformabilities that are nearly identical across the observed range of neutron star masses.

While this degeneracy may limit the ability of the current GW detectors to infer some classes of phase transitions from GW data in the absence of informative priors, we have shown that XG detectors will potentially have the sensitivity to resolve this degeneracy, depending on the neutron star mass distribution and merger rate. These results thus provide additional motivation for the construction of XG facilities such as Einstein Telescope [112], Cosmic Explorer [73], or NEMO [113].

Adopting stronger input from nuclear theory can also help to resolve the degeneracy between certain classes of these models. Thus, continued advances in nuclear theoretical constraints—in particular, around nuclear saturation [114,115]—will also help to provide further constraints on these tidal deformability doppelgängers.

The authors thank Gabriele Bozzola, Katerina Chatziioannou, Pierre Christian, Phil Landry, Feryal Özel, Dimitrios Psaltis, Jocelyn Read, Ingo Tews, and Nicolas Yunes for insightful comments on this work. The authors gratefully acknowledge support from postdoctoral fellowships at the Princeton Center for Theoretical Science, the Princeton Gravity Initiative, and the Institute for Advanced Study. C. A. R. additionally acknowledges support as a John N. Bahcall Fellow at the Institute for Advanced Study. This work was performed in part at the Aspen Center for Physics, which is supported by National Science Foundation (NSF) Grant No. PHY-1607611. E. R. M. acknowledges support for compute time allocations on the NSF Frontera supercomputer under Grant No. AST21006. This work used the Extreme Science and Engineering Discovery Environment (XSEDE) [116] through Expanse at SDSC and Bridges-2 at PSC through allocations PHY210053 and PHY210074. The simulations were also in part performed on computational resources managed and supported by Princeton Research Computing, a consortium of groups including the Princeton Institute for Computational Science and Engineering (PICSciE) and the Office of Information Technology's High Performance Computing Center and Visualization Laboratory at Princeton University. The authors also acknowledge the use of high-performance computing at the Institute for Advanced Study.

*craithel@ias.edu
†emost@princeton.edu

[1] M. Agathos, J. Meidam, W. Del Pozzo, T. G. F. Li, M. Tompitak, J. Veitch, S. Vitale, and C. Van Den Broeck, Phys. Rev. D **92**, 023012 (2015).
[2] C. A. Raithel, Eur. Phys. J. A **55**, 80 (2019).
[3] L. Baiotti, Prog. Part. Nucl. Phys. **109**, 103714 (2019).
[4] K. Chatziioannou, Phys. Rev. D **105**, 084021 (2022).
[5] E. Annala, T. Gorda, A. Kurkela, and A. Vuorinen, Phys. Rev. Lett. **120**, 172703 (2018).
[6] D. Radice, A. Perego, F. Zappa, and S. Bernuzzi, Astrophys. J. Lett. **852**, L29 (2018).
[7] A. Bauswein, O. Just, H.-T. Janka, and N. Stergioulas, Astrophys. J. Lett. **850**, L34 (2017).
[8] E. R. Most, L. R. Weih, L. Rezzolla, and J. Schaffner-Bielich, Phys. Rev. Lett. **120**, 261103 (2018).
[9] B. P. Abbott *et al.* (LIGO Scientific, Virgo Collaborations), Phys. Rev. Lett. **121**, 161101 (2018).
[10] C. Raithel, F. Özel, and D. Psaltis, Astrophys. J. Lett. **857**, L23 (2018).
[11] S. De, D. Finstad, J. M. Lattimer, D. A. Brown, E. Berger, and C. M. Biwer, Phys. Rev. Lett. **121**, 091102 (2018); **121**, 259902(E) (2018).
[12] K. Chatziioannou, C.-J. Haster, and A. Zimmerman, Phys. Rev. D **97**, 104036 (2018).
[13] Z. Carson, A. W. Steiner, and K. Yagi, Phys. Rev. D **99**, 043010 (2019).
[14] B. P. Abbott *et al.* (LIGO Scientific, Virgo Collaborations), Phys. Rev. X **9**, 011001 (2019).

[15] Z. Carson, K. Chatziioannou, C.-J. Haster, K. Yagi, and N. Yunes, Phys. Rev. D **99**, 083016 (2019).
[16] K. Yagi and N. Yunes, Classical Quantum Gravity **33**, 13LT01 (2016).
[17] K. Yagi and N. Yunes, Phys. Rep. **681**, 1 (2017).
[18] T. Zhao and J. M. Lattimer, Phys. Rev. D **98**, 063020 (2018).
[19] G. Pratten, P. Schmidt, and N. Williams, Phys. Rev. Lett. **129**, 081102 (2022).
[20] R. Gamba and S. Bernuzzi, Phys. Rev. D **107**, 044014 (2023).
[21] V. Paschalidis, K. Yagi, D. Alvarez-Castillo, D. B. Blaschke, and A. Sedrakian, Phys. Rev. D **97**, 084038 (2018).
[22] J.-E. Christian, A. Zacchi, and J. Schaffner-Bielich, Phys. Rev. D **99**, 023009 (2019).
[23] V. Dexheimer, R. de Oliveira Gomes, S. Schramm, and H. Pais, J. Phys. G **46**, 034002 (2019).
[24] S. Han and A. W. Steiner, Phys. Rev. D **99**, 083014 (2019).
[25] M. Sieniawska, W. Turczanski, M. Bejger, and J. L. Zdunik, Astron. Astrophys. **622**, A174 (2019).
[26] K. Chatziioannou and S. Han, Phys. Rev. D **101**, 044019 (2020).
[27] H. Tan, V. Dexheimer, J. Noronha-Hostler, and N. Yunes, Phys. Rev. Lett. **128**, 161101 (2022).
[28] S. Bogdanov *et al.*, in 2022 Snowmass Summer Study (2022), arXiv:2209.07412.
[29] A. Gezerlis, I. Tews, E. Epelbaum, S. Gandolfi, K. Hebeler, A. Nogga, and A. Schwenk, Phys. Rev. Lett. **111**, 032501 (2013).
[30] J. E. Lynn, I. Tews, J. Carlson, S. Gandolfi, A. Gezerlis, K. E. Schmidt, and A. Schwenk, Phys. Rev. Lett. **116**, 062501 (2016).
[31] I. Tews, S. Gandolfi, A. Gezerlis, and A. Schwenk, Phys. Rev. C **93**, 024305 (2016).
[32] C. Drischler, K. Hebeler, and A. Schwenk, Phys. Rev. Lett. **122**, 042501 (2019).
[33] C. A. Raithel, F. Özel, and D. Psaltis, Astrophys. J. **844**, 156 (2017).
[34] A. Akmal, V. R. Pandharipande, and D. G. Ravenhall, Phys. Rev. C **58**, 1804 (1998).
[35] B. Margalit and B. D. Metzger, Astrophys. J. Lett. **850**, L19 (2017).
[36] L. Rezzolla, E. R. Most, and L. R. Weih, Astrophys. J. Lett. **852**, L25 (2018).
[37] M. Ruiz, S. L. Shapiro, and A. Tsokaros, Phys. Rev. D **97**, 021501(R) (2018).
[38] M. Shibata, E. Zhou, K. Kiuchi, and S. Fujibayashi, Phys. Rev. D **100**, 023015 (2019).
[39] A. Nathanail, E. R. Most, and L. Rezzolla, Astrophys. J. Lett. **908**, L28 (2021).
[40] F. Özel and P. Freire, Annu. Rev. Astron. Astrophys. **54**, 401 (2016).
[41] M. C. Miller *et al.*, Astrophys. J. Lett. **887**, L24 (2019).
[42] T. E. Riley *et al.*, Astrophys. J. Lett. **887**, L21 (2019).
[43] G. Raaijmakers *et al.*, Astrophys. J. Lett. **887**, L22 (2019).
[44] G. Raaijmakers *et al.*, Astrophys. J. Lett. **893**, L21 (2020).
[45] M. C. Miller *et al.*, Astrophys. J. Lett. **918**, L28 (2021).
[46] T. E. Riley *et al.*, Astrophys. J. Lett. **918**, L27 (2021).
[47] G. Raaijmakers, S. K. Greif, K. Hebeler, T. Hinderer, S. Nissanke, A. Schwenk, T. E. Riley, A. L. Watts, J. M. Lattimer, and W. C. G. Ho, Astrophys. J. Lett. **918**, L29 (2021).
[48] K. Chatziioannou, Gen. Relativ. Gravit. **52**, 109 (2020).
[49] J. G. Martinez, K. Stovall, P. C. C. Freire, J. S. Deneva, F. A. Jenet, M. A. McLaughlin, M. Bagchi, S. D. Bates, and A. Ridolfi, Astrophys. J. **812**, 143 (2015).
[50] H. T. Cromartie *et al.* (NANOGrav Collaboration), Nat. Astron. **4**, 72 (2019).
[51] E. Fonseca *et al.*, Astrophys. J. Lett. **915**, L12 (2021).
[52] B. P. Abbott *et al.* (LIGO Scientific, Virgo Collaborations), Phys. Rev. Lett. **119**, 161101 (2017).
[53] See Supplemental Material at http://link.aps.org/supplemental/10.1103/PhysRevLett.130.201403 for additional details, which includes Refs. [54–70].
[54] J. S. Read, B. D. Lackey, B. J. Owen, and J. L. Friedman, Phys. Rev. D **79**, 124032 (2009).
[55] F. Ozel and D. Psaltis, Phys. Rev. D **80**, 103003 (2009).
[56] C. A. Raithel, F. Ozel, and D. Psaltis, Astrophys. J. **831**, 44 (2016).
[57] A. W. Steiner, M. Hempel, and T. Fischer, Astrophys. J. **774**, 17 (2013).
[58] C. Raithel, P. Espino, and V. Paschalidis, Mon. Not. R. Astron. Soc. **516**, 4792 (2022).
[59] A. S. Schneider, L. F. Roberts, and C. D. Ott, Phys. Rev. C **96**, 065802 (2017).
[60] M. D. Duez, Y. T. Liu, S. L. Shapiro, and B. C. Stephens, Phys. Rev. D **72**, 024028 (2005).
[61] M. Shibata and Y.-i. Sekiguchi, Phys. Rev. D **72**, 044014 (2005).
[62] D. Hilditch, S. Bernuzzi, M. Thierfelder, Z. Cao, W. Tichy, and B. Brugmann, Phys. Rev. D **88**, 084057 (2013).
[63] S. Bernuzzi and D. Hilditch, Phys. Rev. D **81**, 084003 (2010).
[64] M. H. Ruffert, H. T. Janka, and G. Schaefer, Astron. Astrophys. **311**, 532 (1996).
[65] S. Rosswog and M. Liebendoerfer, Mon. Not. R. Astron. Soc. **342**, 673 (2003).
[66] F. Loffler *et al.*, Classical Quantum Gravity **29**, 115001 (2012).
[67] E. Schnetter, S. H. Hawley, and I. Hawke, Classical Quantum Gravity **21**, 1465 (2004).
[68] K. Kiuchi, K. Kawaguchi, K. Kyutoku, Y. Sekiguchi, M. Shibata, and K. Taniguchi, Phys. Rev. D **96**, 084060 (2017).
[69] F. Foucart *et al.*, Phys. Rev. D **99**, 044008 (2019).
[70] K. Kiuchi, K. Kawaguchi, K. Kyutoku, Y. Sekiguchi, and M. Shibata, Phys. Rev. D **101**, 084006 (2020).
[71] H. Jeffreys, *Theory of Probability*, 3rd ed. (Oxford, Oxford, England, 1961).
[72] R. Gamba, J. S. Read, and L. E. Wade, Classical Quantum Gravity **37**, 025008 (2020).
[73] D. Reitze *et al.*, Bull. Am. Astron. Soc. **51**, 035 (2019).
[74] T. Kojo, P. D. Powell, Y. Song, and G. Baym, Phys. Rev. D **91**, 045003 (2015).
[75] G. Baym, T. Hatsuda, T. Kojo, P. D. Powell, Y. Song, and T. Takatsuka, Rep. Prog. Phys. **81**, 056902 (2018).
[76] D. Blaschke and N. Chamel, Astrophysics and Space Science Library **457**, 337 (2018).

[77] C. A. Raithel and E. R. Most, arXiv:2208.04295.
[78] M. Wijngaarden, K. Chatziioannou, A. Bauswein, J. A. Clark, and N. J. Cornish, Phys. Rev. D **105**, 104019 (2022).
[79] M. Breschi, R. Gamba, S. Borhanian, G. Carullo, and S. Bernuzzi, arXiv:2205.09979.
[80] H. Yu, D. Martynov, R. X. Adhikari, and Y. Chen, Phys. Rev. D **106**, 063017 (2022).
[81] A. Bauswein, H. T. Janka, K. Hebeler, and A. Schwenk, Phys. Rev. D **86**, 063001 (2012).
[82] K. Takami, L. Rezzolla, and L. Baiotti, Phys. Rev. D **91**, 064001 (2015).
[83] K. Takami, L. Rezzolla, and L. Baiotti, Phys. Rev. Lett. **113**, 091104 (2014).
[84] L. Baiotti and L. Rezzolla, Rep. Prog. Phys. **80**, 096901 (2017).
[85] V. Paschalidis and N. Stergioulas, Living Rev. Relativity **20**, 7 (2017).
[86] L. Rezzolla and K. Takami, Phys. Rev. D **93**, 124051 (2016).
[87] A. Bauswein and N. Stergioulas, J. Phys. G **46**, 113002 (2019).
[88] S. Bernuzzi, Gen. Relativ. Gravit. **52**, 108 (2020).
[89] D. Radice, S. Bernuzzi, and A. Perego, Annu. Rev. Nucl. Part. Sci. **70**, 95 (2020).
[90] S. Vretinaris, N. Stergioulas, and A. Bauswein, Phys. Rev. D **101**, 084039 (2020).
[91] C. A. Raithel and E. R. Most, Astrophys. J. Lett. **933**, L39 (2022).
[92] E. R. Most, L. J. Papenfort, V. Dexheimer, M. Hanauske, S. Schramm, H. Stöcker, and L. Rezzolla, Phys. Rev. Lett. **122**, 061101 (2019).
[93] A. Bauswein, Niels-Uwe F. Bastian, D. B. Blaschke, K. Chatziioannou, J. A. Clark, T. Fischer, and M. Oertel, Phys. Rev. Lett. **122**, 061102 (2019).
[94] L. R. Weih, M. Hanauske, and L. Rezzolla, Phys. Rev. Lett. **124**, 171103 (2020).
[95] E. R. Most, L. Jens Papenfort, V. Dexheimer, M. Hanauske, H. Stoecker, and L. Rezzolla, Eur. Phys. J. A **56**, 59 (2020).
[96] A. Prakash, D. Radice, D. Logoteta, A. Perego, V. Nedora, I. Bombaci, R. Kashyap, S. Bernuzzi, and A. Endrizzi, Phys. Rev. D **104**, 083029 (2021).
[97] A. Kedia, H. I. Kim, I.-S. Suh, and G. J. Mathews, Phys. Rev. D **106**, 103027 (2022).
[98] Y.-J. Huang, L. Baiotti, T. Kojo, K. Takami, H. Sotani, H. Togashi, T. Hatsuda, S. Nagataki, and Y.-Z. Fan, Phys. Rev. Lett. **129**, 181101 (2022).
[99] C. A. Raithel, F. Ozel, and D. Psaltis, Astrophys. J. **875**, 12 (2019).
[100] E. R. Most and C. A. Raithel, Phys. Rev. D **104**, 124012 (2021).
[101] E. R. Most, L. J. Papenfort, and L. Rezzolla, Mon. Not. R. Astron. Soc. **490**, 3588 (2019).
[102] Z. B. Etienne, V. Paschalidis, R. Haas, P. Mösta, and S. L. Shapiro, Classical Quantum Gravity **32**, 175009 (2015).
[103] M. Breschi, S. Bernuzzi, F. Zappa, M. Agathos, A. Perego, D. Radice, and A. Nagar, Phys. Rev. D **100**, 104029 (2019).
[104] M. Breschi, S. Bernuzzi, K. Chakravarti, A. Camilletti, A. Prakash, and A. Perego, arXiv:2205.09112.
[105] A. Bauswein, H. T. Janka, and R. Oechslin, Phys. Rev. D **82**, 084043 (2010).
[106] A. Figura, J. J. Lu, G. F. Burgio, Z. H. Li, and H. J. Schulze, Phys. Rev. D **102**, 043006 (2020).
[107] C. A. Raithel, V. Paschalidis, and F. Özel, Phys. Rev. D **104**, 063016 (2021).
[108] M. G. Alford, L. Bovard, M. Hanauske, L. Rezzolla, and K. Schwenzer, Phys. Rev. Lett. **120**, 041101 (2018).
[109] E. R. Most, S. P. Harris, C. Plumberg, M. G. Alford, J. Noronha, J. Noronha-Hostler, F. Pretorius, H. Witek, and N. Yunes, Mon. Not. R. Astron. Soc. **509**, 1096 (2021).
[110] D. Radice, S. Bernuzzi, A. Perego, and R. Haas, Mon. Not. R. Astron. Soc. **512**, 1499 (2022).
[111] E. R. Most, A. Haber, S. P. Harris, Z. Zhang, M. G. Alford, and J. Noronha, arXiv:2207.00442.
[112] M. Punturo *et al.*, Classical Quantum Gravity **27**, 194002 (2010).
[113] K. Ackley *et al.*, Pub. Astron. Soc. Aust. **37**, e047 (2020).
[114] C. Drischler, J. W. Holt, and C. Wellenhofer, Annu. Rev. Nucl. Part. Sci. **71**, 403 (2021).
[115] I. Tews *et al.*, Few Body Syst. **63**, 67 (2022).
[116] J. Towns *et al.*, Comput. Sci. Eng. **16**, 62 (2014).